

AD-A 196 470

**DTIC FILE COPY**

(4) (A)

**ADVANCED ARTIFICIAL DIELECTRIC MATERIALS  
FOR MILLIMETER WAVELENGTH APPLICATIONS**

**Annual Technical Report, Part A**

**Contract No. N00014-83-C-0447**

**DTIC  
ELECTE  
JUN 06 1988  
S D**

**ISRAEL S. JACOBS**

**General Electric Company  
Corporate Research and Development  
P.O. Box 8  
Schenectady, New York 12301**

**Report Period 1 Oct 1985 - 30 Jun 1987**

**Prepared for**

**Office of Naval Research  
800 North Quincy Street  
Arlington, Virginia 22217**

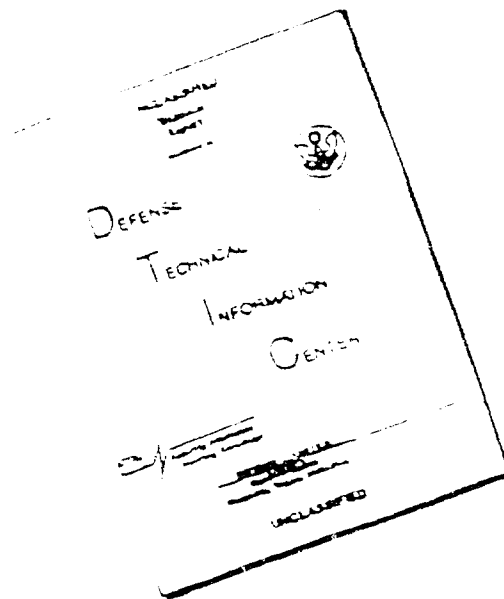
**DISTRIBUTION STATEMENT A**

**Approved for public release  
Distribution Unlimited**

**88-SRD-007**

**88 5 27 09 7**

# DISCLAIMER NOTICE



THIS DOCUMENT IS BEST  
QUALITY AVAILABLE. THE COPY  
FURNISHED TO DTIC CONTAINED  
A SIGNIFICANT NUMBER OF  
PAGES WHICH DO NOT  
REPRODUCE LEGIBLY.

UNCLASSIFIED

SECURITY CLASSIFICATION OF THIS PAGE

A DA 196470

## REPORT DOCUMENTATION PAGE

1a. REPORT SECURITY CLASSIFICATION Unclassified		1b. RESTRICTIVE MARKINGS	
2a. SECURITY CLASSIFICATION AUTHORITY		3. DISTRIBUTION/AVAILABILITY OF REPORT Reproduction in whole or in part is permitted for any purposes by the United States Government	
7a. DECLASSIFICATION/DOWNGRADING SCHEDULE		5. MONITORING ORGANIZATION REPORT NUMBER(S)	
4. PERFORMING ORGANIZATION REPORT NUMBER(S) 88-SRD-007		7b. NAME OF MONITORING ORGANIZATION Office of Naval Research - Code 1131	
6a. NAME OF PERFORMING ORGANIZATION General Electric Company Corporate Research & Develop.	6b. OFFICE SYMBOL (If applicable)	7c. ADDRESS (City, State and ZIP Code) 800 N. Quincy Street Arlington, VA 22217	
6c. ADDRESS (City, State and ZIP Code) PO Box 8 Schenectady, NY 12301		8. PROCUREMENT INSTRUMENT IDENTIFICATION NUMBER N 00014-83-C-0447	
8a. NAME OF FUNDING/SPONSORING ORGANIZATION	8b. OFFICE SYMBOL (If applicable)	10. SOURCE OF FUNDING NOS.	
8c. ADDRESS (City, State and ZIP Code)		PROGRAM ELEMENT NO. 61153N	TASK NO. OC
11. TITLE (Include Security Classification) Advanced Artificial Dielectric Materials (U)		PROJECT NO. RR02202	WORK UNIT NO.
12. PERSONAL AUTHOR(S) Jacobs, Israel S.			
13a. TYPE OF REPORT Annual Report	13b. TIME COVERED FROM 86OCT01 TO 87JUN30	14. DATE OF REPORT (Yr., Mo., Day) 88APR01	15. PAGE COUNT 35
16. SUPPLEMENTARY NOTATION Full Title of Contract: Advanced Artificial Dielectric Materials for Millimeter Wavelength Applications			
17. COSATI CODES		18. SUBJECT TERMS (Continue on reverse if necessary and identify by block number)	
FIELD	GROUP	SUB. GR.	
		Artificial Dielectrics, Induced Magnetic Permeability, Permittivity Models for Random Arrays, Effect of Binder Permittivity	
19. ABSTRACT (Continue on reverse if necessary and identify by block number) This is Part A of a two-part Annual Report. (Part B is classified.) This part describes a continuation and completion of work on non-magnetic composite artificial dielectrics. The electromagnetic evaluation of polymer-based composites was improved in the region of 2-18 GHz and extended to include K <sub>6</sub> (26-40 GHz) and W (75-110 GHz) bands, through cooperation at NRL. Permittivity variations with frequency were essentially negligible. Induced permeability results were significant and were consistent with calculated models and data of earlier parts of this program. Previous results for permittivity versus volume loading were reinforced. The effect of binder permittivity was studied using an alternative inorganic binder. Qualitatively similar results were found, which scaled reasonably well to the binder permittivity as predicted. The permittivity behavior versus volume loading for randomly packed artificial dielectrics was modeled empirically from several ideal experiments and theoretically from a simplified pair-interaction model. The convergence of experiments on themselves and with the simplified model yields a satisfactory predictive control in considering the properties of such artificial dielectric materials.			
20. DISTRIBUTION/AVAILABILITY OF ABSTRACT UNCLASSIFIED/UNLIMITED <input type="checkbox"/> SAME AS RPT. <input checked="" type="checkbox"/> DTIC USERS <input type="checkbox"/>		21. ABSTRACT SECURITY CLASSIFICATION Unclassified	
22a. NAME OF RESPONSIBLE INDIVIDUAL Dr. D.E. Polk (ONR)		22b. TELEPHONE NUMBER (Include Area Code) (202) 696-4401	22c. OFFICE SYMBOL Code 1131 M

# TABLE OF CONTENTS

Section	Page
PREFACE .....	1
SUMMARY .....	3
I INTRODUCTION .....	5
II POLYMERIC BINDER COMPOSITE DIELECTRIC .....	6
II.1 Improved Evaluation at Centimeter Wavelengths .....	6
II.2 Evaluation Efforts at Millimeter Wavelengths .....	8
III PERMITTIVITY EFFECTS: ALTERNATIVE INORGANIC BINDER .....	10
III.1 High-frequency Permittivity Measurements .....	15
III.2 High-frequency Permeability Measurements .....	15
IV IMPROVED MODELING OF RANDOMLY PACKED ARTIFICIAL DIELECTRICS .....	18
IV.1 Pair Interactions in Artificial Dielectric Media (W.T. Doyle) .....	21
IV.1.1 Introduction .....	21
IV.1.2 Clustering Effects .....	21
IV.1.3 Pair Polarizabilities .....	23
IV.1.4 Dielectric Constant .....	24
IV.1.5 Comparison with Experiment .....	27
IV.1.6 Conclusions .....	29
IV.2 Further Experimental Comparisons with Theoretical Models .....	29
V CONCLUSIONS .....	30
REFERENCES .....	33



Accession For	
NTIS GRA&I	✓
DTIC TAB	✓
Unannounced	✓
Justification	
By <i>per-etr</i>	
Distribution	
Availability	
Dist	
A-1	

# LIST OF ILLUSTRATIONS

Figure	Page
1 Example of constitutive parameter data obtained on the HP 8510 Network Analyzer at NRL for sample No 2, $p = 0.41$ , $20 \mu\text{m} < d < 37 \mu\text{m}$ .....	7
2 Example of same data on toroid as obtained on the HP 8510B Network Analyzer ....	7
3 Relative permittivity, $\epsilon_r'$ , vs volume loading, $p$ , for $\text{Ni}_{92}\text{Cr}_8$ alloy at various particle sizes in polyurethane composites .....	9
4 Permittivity and permeability vs frequency in W-band for $\text{Ni}_{92}\text{Cr}_8$ alloy powder ( $20 \mu\text{m} < d < 37 \mu\text{m}$ ) in polyurethane, $p = 0.39$ .....	9
5 Permittivity and permeability vs frequency in $K_\alpha$ -band for $\text{Ni}_{92}\text{Cr}_8$ alloy powder ( $20 \mu\text{m} < d < 37 \mu\text{m}$ ) in polyurethane, $p = 0.42$ .....	11
6 Comparison of experiment and model calculations: $\mu_r'$ vs frequency, $p = 0.1$ , for $\text{Ni}_{92}\text{Cr}_8$ alloy powder in polyurethane .....	11
7 Comparison of experiment and model calculations: $\mu_r'$ vs frequency, $p = 0.2$ .....	12
8 Comparison of experiment and model calculations: $\mu_r'$ vs frequency, $p = 0.3$ .....	12
9 Comparison of experiment and model calculations: $\mu_r'$ vs frequency, $p = 0.4$ .....	12
10 Comparison of experiment and model calculations: $\mu_r''$ vs frequency, $p = 0.1$ .....	13
11 Comparison of experiment and model calculations: $\mu_r''$ vs frequency, $p = 0.2$ .....	13
12 Comparison of experiment and model calculations: $\mu_r''$ vs frequency, $p = 0.3$ .....	14
13 Comparison of experiment and model calculations: $\mu_r''$ vs frequency, $p = 0.4$ .....	14
14 Relative permittivity, $\epsilon_r'$ , vs volume loading, $p$ , for $\text{Ni}_{92}\text{Cr}_8$ alloy, $10 \mu\text{m} < d < 20 \mu\text{m}$ , in lead-solder glass binder, measured at 35 GHz .....	17
15 Scaled comparison of permittivity behavior, $\epsilon_c'/\epsilon_b'$ , at 35 GHz, for artificial dielectrics with two different binders .....	17
16 Comparison of experiment and model calculations: $\mu_r'$ and $\mu_r''$ vs frequency, various loadings; for $\text{Ni}_{92}\text{Cr}_8$ alloy powder, $10 \mu\text{m} < d < 20 \mu\text{m}$ , in lead-solder glass .....	19
17 Comparison of classical dielectric models of percolating vs non-percolating systems	20
18 Comparison of an actual composite: Ni-Cr/polyurethane, $p = 0.1$ , $20 \mu\text{m} < d < 37 \mu\text{m}$ , SEM of cold-microtomed sample .....	22
19 Incremental polarizabilities, $\alpha_{12}$ , vs separation parameter $x = r/2R$ .....	26
20 Dielectric constant, $\epsilon_r'$ , vs volume loading, $p$ . Calculated models with and without pairing, $n_2$ .....	28
21 Reduced permittivity, $\epsilon'/\epsilon_b'$ , vs volume loading, $p$ .....	28
22 Reduced permittivity or conductance data from several ideal experiments compared with several multipole models and the classical dipole model .....	31
23 Calculated model behaviors of permittivity vs volume loading, compared with averaged data from microwave experiments on solid metal powders .....	31

## LIST OF TABLES

Table	Page
1 Thermomagnetic evaluation parameters of inorganic composites used for electromagnetic study .....	16
2 Incremental polarizabilities, $\alpha_{12}$ , per pair as a function of the separation parameter, $x = r/2R$ .....	25

## PREFACE

This report was prepared by General Electric Corporate Research and Development under ONR Contract No. N00014-83-C-0447. The Principal Investigator was Dr. Israel S. Jacobs of the Materials Research Program, Electronics Materials Laboratory. There were a number of major collaborators in this effort and they are identified in the Introduction.

The program was administered under the direction of Dr. Donald E. Polk, Code 1131M of the Materials Division of the Office of Naval Research, Arlington, VA, 22217.

## SUMMARY

This program is concerned with the development of a novel class of artificial dielectrics and a deeper understanding of its properties at millimeter wavelengths. The work is divided between two subclasses, one of essentially non-magnetic composite dielectrics, Part A, and one of composite magneto-dielectrics, Part B. Inasmuch as some aspects of the latter group are classified, this third (extended) annual report (for the period 1 Oct 1985 to 30 June 1987) appears in two sections of which this is Part A (unclassified). In this report period we have completed the tasks of the contract work statement dealing with the non-magnetic artificial dielectric composites.

We have improved the electromagnetic evaluation of polymeric binder artificial composites in the centimeter wavelength range, 2-18 GHz, through collaboration with Naval Research Lab staff. Our earlier work at 35 GHz in the millimeter wavelength region on such composites has been extended (at NRL) into both the  $K_a$ -band (26-40 GHz) and the W-band (75-110 GHz). Permittivity results changed but little over the full range covered. However, the induced permeability results showed variations with frequency and size which are consistent with the calculations and early data presented in prior reports in this program. This success provides a foundation for working with the more difficult metallic magneto-dielectrics.

Permittivity behavior focusses on the packing dependence and the scaling properties with change of binder. The former behavior was sketched in the earlier stages and was well corroborated in the present phase. Experiments with an alternative inorganic binder show qualitatively similar behavior to the polymer binder, but with higher dielectric constants. When scaled to binder permittivity, the two systems agree satisfactorily at low packing, with deviations at higher values attributed to alloy particle distortion during inorganic composite preparation.

Modeling the permittivity behavior of these randomly packed artificial dielectrics is another success in this period. Ideal experiments in the literature on fluid systems provide an empirical reference model which some of our data resemble. A rather simple pair-interaction model, developed with Prof. W.T. Doyle, comes closer to describing the experimental results than any other model known to us. Although the model is obviously an oversimplification, it illustrates the importance of local clustering and higher order multipole effects. The apparent convergence of experiments, and of experiment and model, result in a satisfactory predictive control in considering the permittivity behavior of this class of artificial dielectrics.



## I. INTRODUCTION

This research focuses on the development of a class of artificial dielectrics and seeks a better understanding of its electromagnetic properties at millimeter wavelengths. This is the third (extended) year of the program. The motivation for this study was derived from a Theoretical Radar Absorbing Materials Model developed by us during a classified program [1]. That study was based on analysis of measurements at microwave frequencies (centimeter wavelengths), albeit with many implications for the millimeter wavelength region. The current program is generally divided between two subclasses, one of essentially nonmagnetic composite dielectrics (unclassified) and one of composite magneto-dielectrics (classified, at least in part). This annual report is thus prepared in two sections, Parts A and B, with the work on magneto-dielectrics appearing in a subsequent *classified* section, Part B.

In the previous stages of this program [2,3] an interesting artificial dielectric was developed. Metallic alloy particles of the composition  $\text{Ni}_{52}\text{Cr}_8$  were prepared by gas-water atomization which left a thin oxide coating for isolation as verified by resistance and Auger electron spectroscopy. The alloy is ferromagnetic below a Curie point of  $\sim 165$  K, which facilitates a magnetic determination of volume loading in composites while retaining the desired nonmagnetic behavior at room temperature. A polymeric binder was used initially, and a successful effort was mounted to develop an alternative inorganic binder. Classical calculations show that induced magnetic dipole effects (eddy currents) depend markedly on the ratio of particle radius to skin depth which in turn depends on frequency and alloy resistivity. The material and measurement parameters of this study span the range of interesting behavior. Initial measurements of the complex permeability of polymeric composites around 10 GHz and at 35 GHz agree rather well with calculations.

An exploration of theoretical descriptions of the dielectric properties of heterogeneous media illustrates why the relatively simple Clausius-Mossotti/Maxwell (C-M/M) calculation is a good starting point for non-percolating systems of the present type. Measurements of permittivity versus volume loading (at 35 GHz) conform generally to the prediction of modern calculation in a smooth departure from the host binder value and in an upward deviation from the classical CM/M calculation. The effects of higher-order multipole interactions and geometrical packing limits as calculated in recent years for regular lattice arrays are thus demonstrated in random composites. However, the upward deviations with increasing volume loading are steeper than predicted, which may be a consequence of local microstructure.

This unclassified portion of the Annual Report covers work described under Tasks 1, 2, 3, and 7 of the original program schedule. Their titles are as follows: Investigate Effect of Binder Permittivity in Artificial Dielectrics, Analyze Effects of Microstructure Control in Passivated Metal-Insulator Composites, Develop Alternative Theoretical Approaches to Composite Dielectrics, and Investigate Millimeter-Wavelength Properties of Artificial Dielectric Composites.

Again this year there were significant inputs to the effort from a number of collaborators and consultants. We are happy to acknowledge them, as listed here with their areas of contribution: For improved measurements at centimeter wavelengths as well as for experiments at millimeter wavelengths, F.J. Rachford, S. Browning and D.W. Forester (Naval Research Laboratory, Washington, D.C.); for microwave measurements at  $K_a$  band, J.O. Hanson (GE-ReEntry Systems Operation, Philadelphia); for preparation of composites with alternative inorganic binder, M.P. Borom and L.E. Szala (GE-CRD); for a wide range of responsibilities with the principal investigator, H.J. Patchen (GE-CRD); for major contributions in the modeling of random artificial dielectrics, Prof. W.T. Doyle (Dartmouth); for general consultations on physics and measurements, Prof. W.P. Wolf (Yale).

## II. POLYMERIC BINDER COMPOSITE DIELECTRIC

In this section we focus on the essentially non-magnetic artificial dielectric prepared with Ni-Cr alloy in a polyurethane polymeric binder as described for previous stages of this program [2,3]. The earlier microwave measurements have been considerably improved and extended as reported below. Measurements on composites with the alternative, higher-permittivity, inorganic binder are discussed in Section III.

### II.1 Improved Evaluation at Centimeter Wavelengths

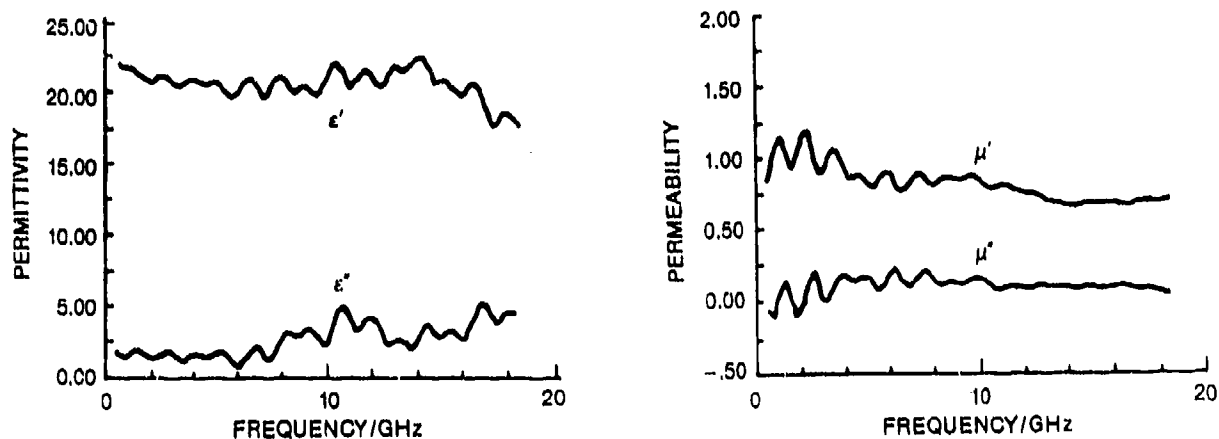
In the preceding reports [2,3] we presented measurement results for the complex constitutive parameters,  $\epsilon'$ ,  $\epsilon''$  (permittivity) and  $\mu'$ ,  $\mu''$  (permeability) for the frequency range, 6-12 GHz, as obtained from a somewhat antiquated Hewlett-Packard Network Analyzer in the Series 8410. During a visit to NRL in November 1985 to discuss millimeter wavelength experiments, we brought our 7-mm diameter coaxial toroids for possible confirmatory measurements on their newer H-P Series 8510 analyzer. Through the cooperation of F.J. Rachford and with the help of S. Browning, it proved possible to measure all eight members of the series (Table 3, Reference 2) from zero volume-loading,  $p$ , up to  $p \sim 0.4$ . In most cases, more than one toroid was measured. The range of measurement was 250 MHz to 18 GHz, but owing to thickness effects, the results were most useful between 2 GHz and 18 GHz.

An example of the quality of this work is shown in Figure 1 for the sample #2, with a volume loading  $p = 0.41$  of alloy particles in the size range  $20 \mu\text{m} < d < 37 \mu\text{m}$ . The whole series was measured in about 4 hours! The overall quantity and quality of the results, when also coupled to the fixed frequency 35 GHz measurements reported in Reference 3, inspired us to present a brief report at the March 1986 meeting of the American Physical Society [4].

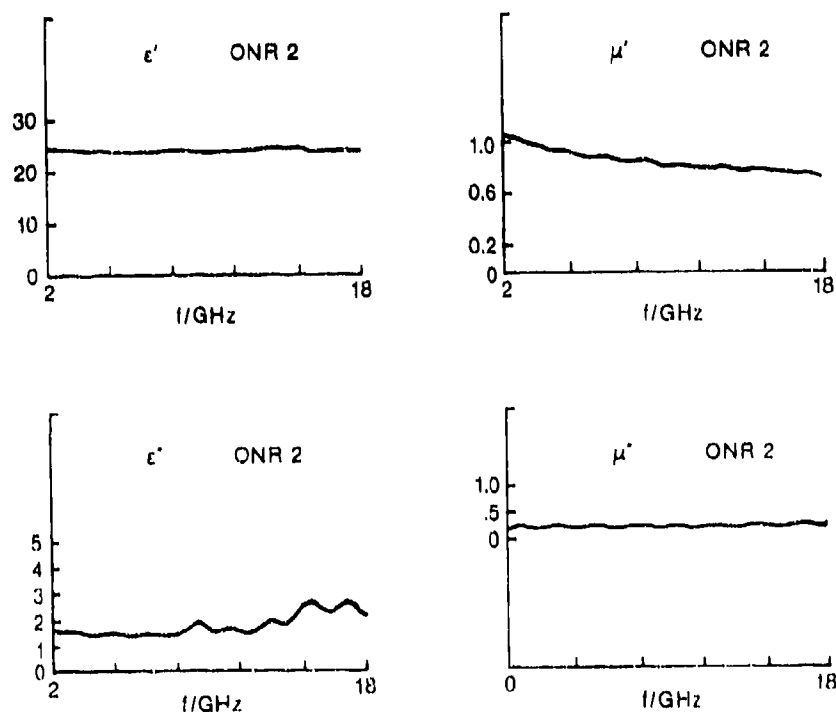
The performance of that instrument left such a profound impression on us that we were able to convince our management to order similar equipment in mid-1987. (This was forced by the terminal illness and breakdown of our older 8410 system.)

We have since come to understand some mildly deprecatory remarks by Rachford and Browning about the quality of their November 1985 data, in response to our joyous praise thereof. Thus we now understand that data acquired more slowly, with repeat data averaging, forward and reverse propagation direction averaging, as well as very careful attention to sample fit and calibrations can produce even better quality data. After the period of this report, we were able to measure one of the original samples on our new H-P 8510-B Network Analyzer. Typical very good results for the same sample #2 are shown in Figure 2. Unfortunately, most of the samples had lost their mechanical integrity by the time of this measurement, so the full series could not easily be repeated. (The polyurethane binder is intended for laboratory model composites and was chosen for ease of fabrication rather than long term durability.) It should be stressed that the showing of comparative data is not done in a sense of competition, but rather to illustrate the potential of the modern instrument.

Combining the NRL results for dielectric behavior, at the selected frequency of 10 GHz, with the GE-RSO results on these composites at 35 GHz (Figure 5 of Reference 3) yields the curve of Figure 3. The agreement between the two sets is generally quite good, reinforcing the conclusions of negligible frequency dependence and independence of particle size. The former conclusion is also rather well supported from Figures 2 and 3 ( $\epsilon'$ , data) over the near-decade of frequencies, 2 to 18 GHz.



1. Example of constitutive parameter data obtained on the HP 8510 Network Analyzer at NRL for sample #2,  $p = 0.41$ ,  $20 \mu\text{m} < d < 37 \mu\text{m}$ .



2. Example of same data as in Figure 1, on toroid from same sample material, as obtained with greater care on the HP 8510B Network Analyzer at GE-CRD.

The data of Figure 2, and for the other samples measured at NRL, enable us to add significantly to our study of the frequency and particle-size dependences of the induced permeability effects in these non-magnetic artificial dielectric composites. (For our earlier results, see Figure 9-16 of Reference 3 and Figure 18-25 of Reference 2.) We defer presenting these results until the next subsection, so as to include the available higher frequency data.

## II.2. Evaluation Efforts at Millimeter Wavelengths

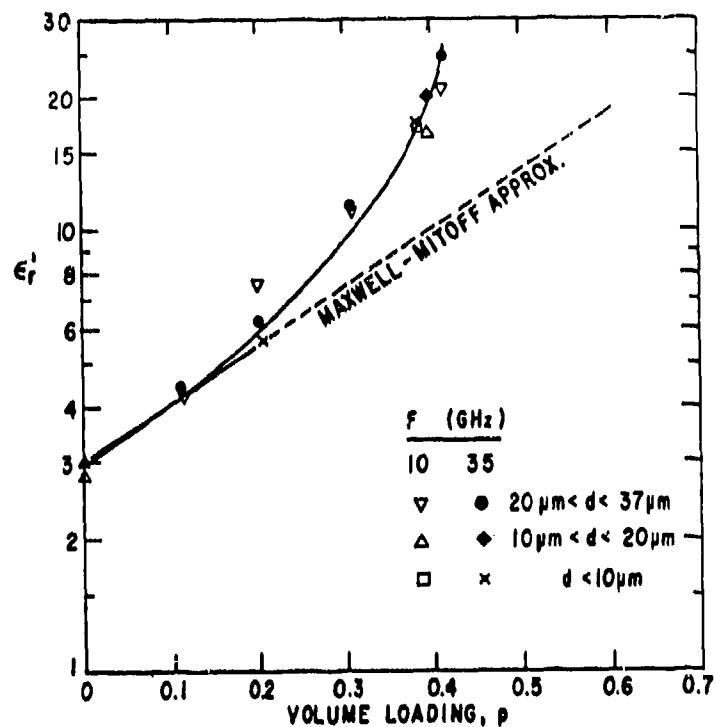
Initial efforts at extending the frequency range of measurements were reported in Reference 3. These were carried out at 35 GHz (fixed frequency) by J.O. Hanson at GE-RSO (Philadelphia) using a slotted line technique with a circular waveguide cavity on some 7 samples (see Figure 3). According to the provisions of the contract, other millimeter wavelength region measurements are to be performed at the Naval Research Laboratory within the limits of their equipment and scheduling. The principal collaborators there are Dr. F.J. Rachford and Dr. D.W. Forester. In Reference 3 we described the preparation and initial characterization of nominal  $p=0.40$  samples for free space (or arch) methods and for waveguide techniques at several bands, e.g.,  $K_\alpha$  (26-40 GHz), Q (40-60 GHz) and W (75-110 GHz). (See Sections II.1 and II.2, Table 1, of Reference 3.)

A considerable effort was expended at NRL on this project by Rachford. Satisfactory results were obtained for the waveguide samples at  $K_\alpha$  band, as judged by consistency with the lower frequency data and the overlapping experiments at 35 GHz by Hanson. Most of the the remaining effort was directed toward obtaining free space transmission on an x-ray diffraction table for fixing the various angles needed in the analysis. The samples had been cut to thickness suitable for W-band. There were a few successes in the W-band range, but when these samples were used at  $K_\alpha$  or Q bands, the results were unsatisfactory.

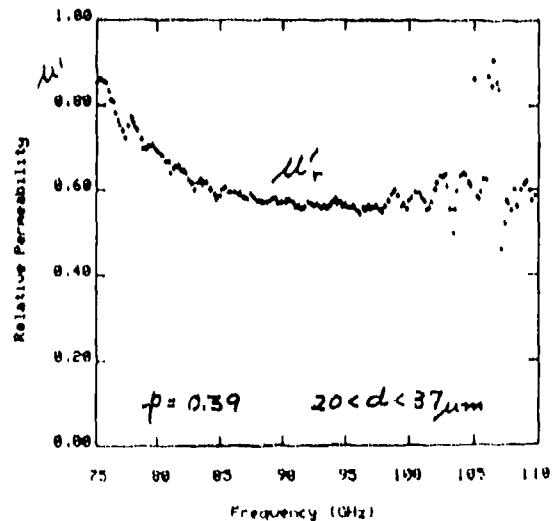
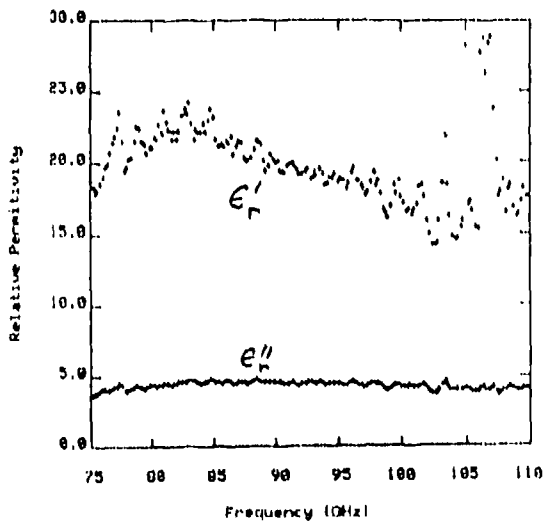
As an example of success at W-band, the data for a  $p=0.39$ ,  $20\ \mu\text{m} < d < 37\ \mu\text{m}$  composite are shown in Figure 4. The permittivity value of about 20 agrees with Figure 3 and the relative permeability of about 0.6 will turn out (below) to fit well with other results. Implicit in the general fit of the permittivity is the condition that the dielectric behavior of the permuthane binder at  $\sim 100$  GHz is essentially the same as at the lower frequencies. This is nicely confirmed by direct measurements at NRL on a polyurethane slab supplied by us. Rachford reports a nearly constant value for  $\epsilon_r'$  of 2.6 when fitting data from 75 to 110 GHz. This is quite close to the lower frequency values of 2.8 and 3.0 previously obtained. If we had full confidence in the accuracy of the slightly lower value, it would imply an 8% reduction in the composite  $\epsilon_r'$  at that frequency relative to a low frequency value. However, such a spread is within the scatter limits of the experimental results.

Returning to the waveguide measurements, several techniques were employed. The "most acceptable" results came from analysis of network analyzer measurements of the amplitude and phase of the transmitted signal  $S_{21}$  for single and double thicknesses. When reflection measurements  $S_{11}$  with and without a short circuit backing were included, there was considerably more frequency dependence to the calculated  $\epsilon$  and  $\mu$  values than with the other experimental set, as well as more than "expected," based on the lower and higher frequency data already explored.

In Figure 5 we show permittivity and permeability results obtained by fitting to the observed  $S_{21}$  parameters for a  $p=0.42$ ,  $20\ \mu\text{m} < d < 37\ \mu\text{m}$  composite sample in the  $K_\alpha$  band. The  $\epsilon_r'$  value of 24.5 is in excellent agreement with results of Figure 3 and the  $\mu_r'$  behavior is also rather satisfactory. A similar success was obtained for the smaller particle,  $d < 10\ \mu\text{m}$ ,  $p=0.36$  sample in this same frequency



3. Relative permittivity,  $\epsilon_r'$ , versus volume loading,  $p$ , for  $\text{Ni}_{92}\text{Cr}_8$  alloy at various particle sizes in polyurethane composites. Data at 10 GHz from NRL and at 35 GHz from GE-RSO.



4. Permittivity and permeability vs frequency in W-band for  $\text{Ni}_{92}\text{Cr}_8$  alloy powder ( $20 \mu\text{m} < d < 37 \mu\text{m}$ ) in polyurethane,  $p=0.39$ , as measured at NRL.

band, from the  $S_{21}$  parameters. Deviations from "perfect" agreement are within the scatter band of general results.

Following these descriptions, we can present the ensemble of permeability data superposed on model calculation [2]. These include the frequency and size dependent results from the 2-18 GHz band (from NRL) in addition to our earlier data [2], the  $K_a$  band and 35 GHz fixed data, and the one data group ( $p=0.4$ ) from W-band (75 to 110 GHz). Loss permeability,  $\mu_r''$ , was not measurable in the NRL experiments. The results and comparisons appear in Figures 6-9 for the real part,  $\mu_r'$ , and in Figures 10-13 for the imaginary (or loss) part,  $\mu_r''$ . While the addition of more results introduces some small confusion and more scatter to these graphs, especially for  $p=0.4$  which embraces most samples, the rough accord between experiment and calculation is preserved for both  $\mu_r'$  and  $\mu_r''$ . The qualitative features are, however, easier to see on the  $\mu_r'$  comparisons, e.g., particle size effects. We can also imagine the possible further improvement that could follow upon further attention to measurement procedures in high quality equipment such as the HP 8510 Network Analyzer (Cf discussion of Figure 1 and 2).

Overall, with the ensemble of data from up to 5 different measurement experiments covering from 2 GHz to 100 GHz, we feel secure with the agreement between model and experiment.

### III. PERMITTIVITY EFFECTS: ALTERNATIVE INORGANIC BINDER

As noted in our earlier reports, especially Reference 3, the dielectric constant of the binder,  $\epsilon_b'$ , is a scaling parameter in the formulas for the composite permittivity,  $\epsilon_c'$ , of artificial dielectrics. In other words,  $\epsilon_b'$  sets the level in a multiplicative way for  $\epsilon_c'$ . For example in the Mitoff approximation to the Maxwell (Clausius-Mossotti) formula [5]:

$$\log \epsilon_c' \approx \log \epsilon_b' + G p$$

or

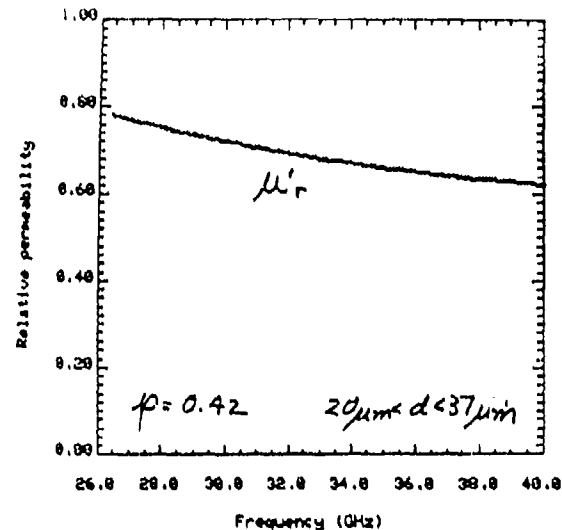
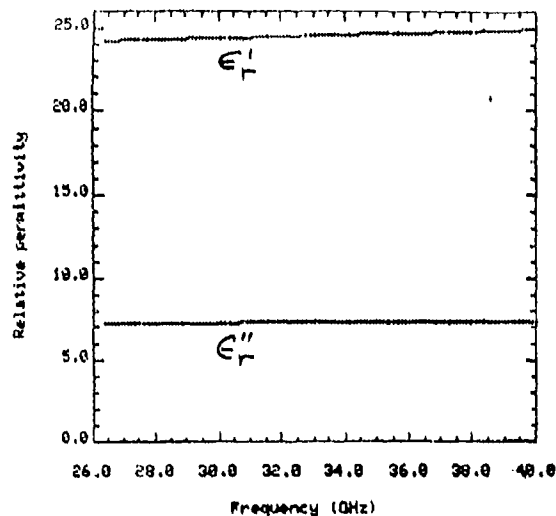
$$\epsilon_c' / \epsilon_b' \approx 10^{Gp},$$

where  $p$  is the volume loading of the metallic particle and  $G$  is a constant of value 1.3. Thus choosing a binder with twice or half the value for  $\epsilon_b'$  is predicted to produce a doubling or halving in the value of  $\epsilon_c'$ . The relevance of this effect lies in its role for the electromagnetic wavelength in the medium, an important parameter in many applications.

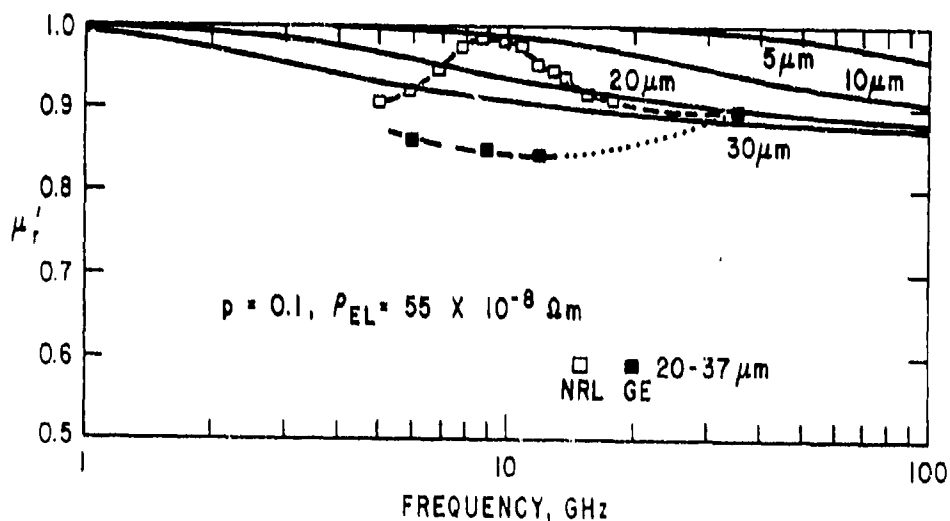
In the original proposal, one of the tasks was to verify this prediction in the microwave and/or millimeter wavelength regions by comparing artificial dielectric composites with two different insulating binders. (In hindsight, the proposed task was rather naive in that the prediction has been rather well established.) Our plan called for one organic, polymeric binder, for which  $\epsilon_b'$  is usually near 3, and a second inorganic binder that could carry an  $\epsilon_b'$  value in the range of 6 to 10.

The search for a suitable inorganic, hopefully high permittivity, binder was more difficult than anticipated. It was documented in our prior report [3]. We settled on a low melting lead-solder glass in a processing procedure chosen to cause least chemical interaction and, at most, minor deformation of the metallic alloy particles. Volume loadings were obtained as before, i.e., measurement of composite Curie temperature (below room temperature,  $\sim 150$  K) along with low temperature (6 K) saturation magnetization.

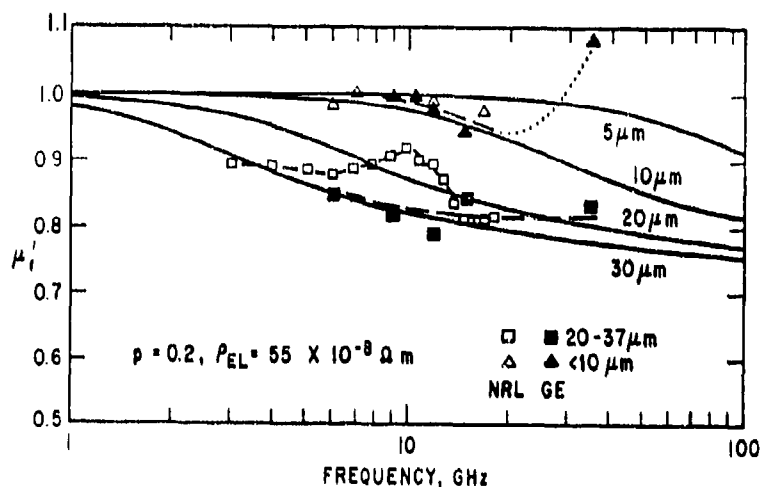
A significant snag developed when it proved essentially impossible to machine satisfactorily precise toroids for coaxial line microwave characterization. We then resorted to fabrication of the



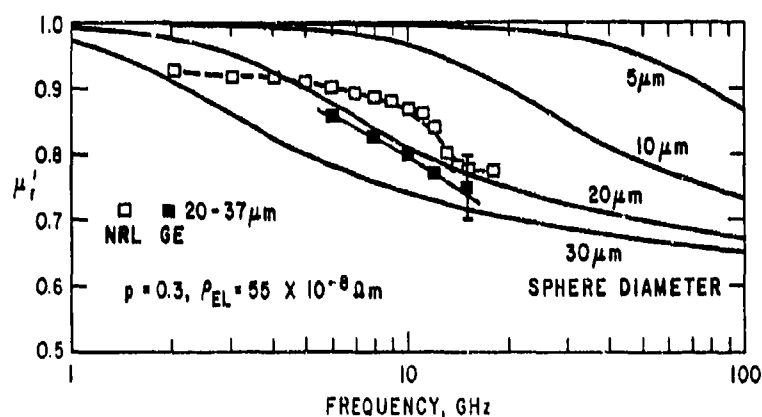
5. Permittivity and permeability vs frequency in K<sub>a</sub>-band for Ni<sub>92</sub>Cr<sub>8</sub> alloy powder (20 μm < d < 37 μm) in polyurethane, p=0.42, as measured by waveguide techniques at NRL.



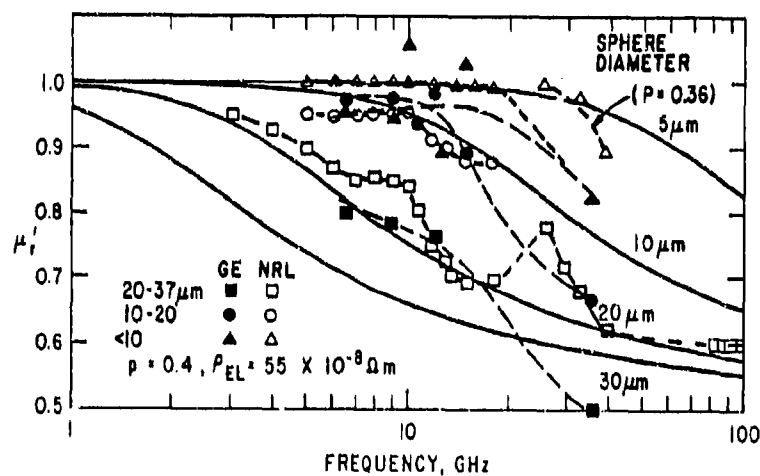
6. Comparison of experiment and model calculations:  $\mu'_r$  vs. frequency,  $p=0.1$ , for Ni<sub>92</sub>Cr<sub>8</sub> alloy powder in polyurethane, from measurements at GE and NRL.



7. Comparison of experiment and model calculations:  $\mu_r$  vs. frequency,  $p=0.2$ ; material system of Figure 6.

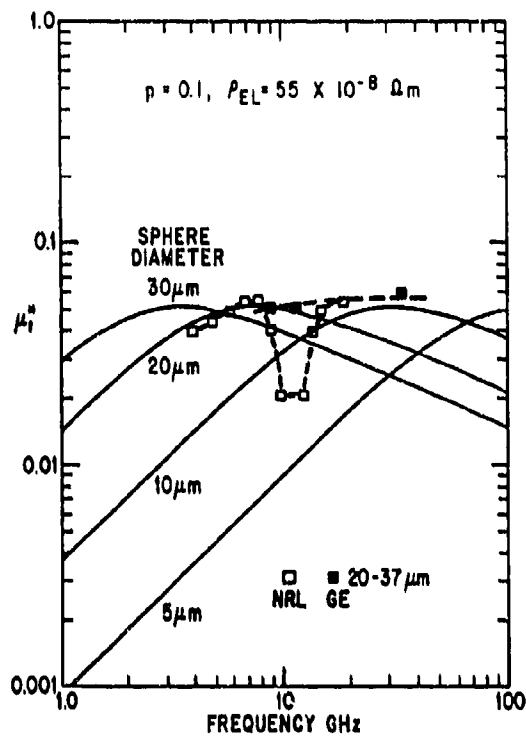


8. Comparison of experiment and model calculations:  $\mu_r$  vs. frequency,  $p=0.3$ , material system of Figure 6.

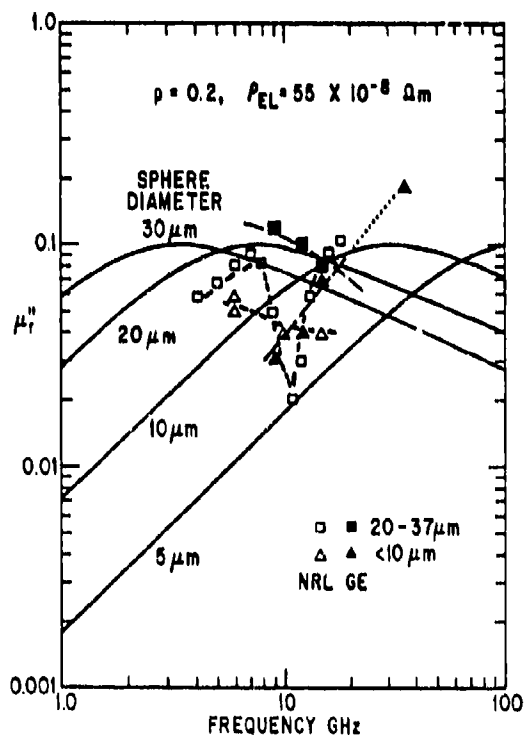


9. Comparison of experiment and model calculations  $\mu_r$  vs. frequency,  $p=0.4$ ; material system of Figure 6.

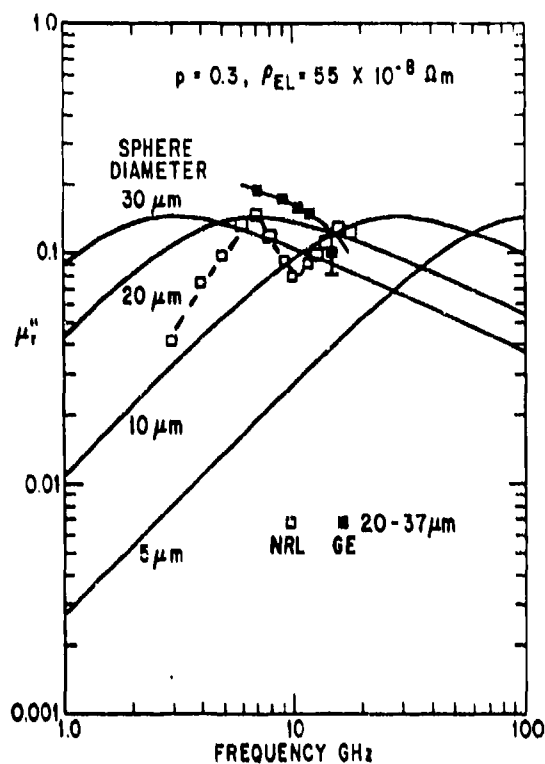




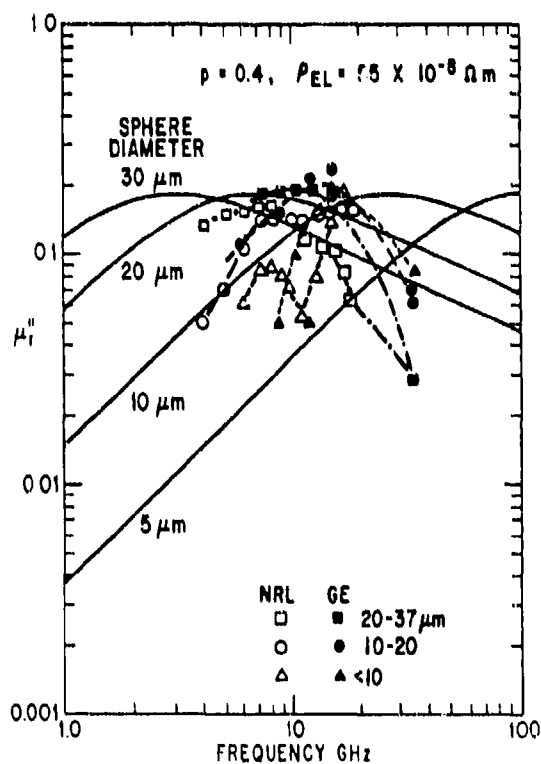
10. Comparison of experiment and model calculations:  $\mu_r''$  vs. frequency,  $p=0.1$ ; material system of Figure 6.



11. Comparison of experiment and model calculations:  $\mu_r''$  vs. frequency,  $p=0.2$ ; material system of Figure 6.



12. Comparison of experiment and model calculations:  $\mu_r''$  vs. frequency,  $p=0.3$ ; material system of Figure 6.



13. Comparison of experiment and model calculations:  $\mu_r''$  vs. frequency,  $p=0.4$ ; material system of Figure 6.

simpler solid disks needed for the slotted-line technique used at the single frequency, 35 GHz, by our colleague J. Hanson at GE-RSO (Philadelphia).

### III.1 High-frequency Permittivity Measurements

A new series of samples was fabricated for these measurements. Their initial characterization parameters are shown in Table 1. Although the least aggressive fabrication procedure of the prior work was that of sintering the  $\text{Ni}_{72}\text{Cr}_8$  alloy powder with the low melting glass, the resulting composites did not have a high density and were still rather weak for subsequent machining. Therefore, a mild hot pressing at relatively low temperature was used for most of the new samples. Based on the early work, this would likely produce slight deformation of the alloy powder, which could influence the electromagnetic results.

Measurements on solid disks were made at 35 GHz for these samples and for the binder glass. The latter exhibited a dielectric constant,  $\epsilon_r'$ , of 8.2, almost three times that of the organic polymer polyurethane. Thus a clear binder permittivity effect should be seen. In Figure 14 we show the results for permittivity versus volume loading,  $\epsilon_r'$  vs.  $p$ , for this series. It should be compared with Figure 3, and the qualitative similarity is obvious.

Next we consider the comparison on a quantitative level, presented in Figure 15. This graph takes  $\epsilon_c'/\epsilon_b'$  for each binder where  $\epsilon_b'$  is 2.8 for the polymer and 8.2 for the glass. At low loadings, up to 20% by volume, the scaled agreement is excellent. There is appreciable deviation at higher  $p$ -values.

A possible reason for the deviation is the enhanced polarizability of non-spherical particles such as might have occurred during the hot-pressing preparation. It should also be recalled that the powder preparation run RS-67 already yielded a modest share of non-spherical "pickle-like" particles as was shown in Figure 17 of Reference 3. A comparative scaled plot of polymer composites of this alloy with one for B-series polymer composites, whose alloy particles are quite spherical, was shown in Figure 8 of Reference 3. The Ni-Cr alloy series (from RS-67) permittivity data had a considerable upward deviation from the behavior of the B-series, even without any possible deformation of the particles in composite preparation. In hindsight, we now attribute that deviation between the two experimental systems to the non-spherical nature of some of the Ni-Cr alloy RS-67 particles. (We note in passing that Figure 15 also includes 35 GHz data from the  $K_a$ -band sweeps at NRL on the two polymeric composites described above in Section II.2 and Figure 5).

To sum up this section, the data of Figure 15 do confirm the role of binder permittivity as a scaling parameter in the dielectric behavior of artificial dielectric composites. We remarked earlier that this has an impact on application design. It also could be relevant for quality control in composites. If there were significant porosity in a particular composite preparation, that could be treated according to mixing rules as a diluent to the binder [5,2] which in turn could lower the final composite permittivity.

### III.2. High-frequency Permeability Measurements

These inorganic composite samples measured at 35 GHz also displayed relevant permeability results, along the lines previously modelled for the polymeric binder composites. Inasmuch as both binders are non-conducting and non-magnetic, ( $\mu_b'' = 1$ ,  $\mu_b' = 0$ ) there are no changes introduced in the expected permeability behavior by changing binder. Since a single particle size group was used for this series,  $10\text{ }\mu\text{m} < d < 20\text{ }\mu\text{m}$ , we make our comparison between experiment and calculation with the expected behavior for  $d = 20\text{ }\mu\text{m}$ . The comparison is shown in Figure 16 for both real and

TABLE 1

**Thermomagnetic Evaluation Parameters of Inorganic Composites  
Used for Electromagnetic Study**

**Material: SG-7 Lead-Solder Glass with RS-67 Run of  $\text{Ni}_{52}\text{Cr}_8$ ,  $10 < d < 20 \mu\text{m}$**

Sample Identity	Nominal Alloy v/o	Curle Temp K	Sat-Mag $\sigma_{\infty}$ (6 K) emu/g	Specific Grav.	Measured Vol. Load p
SG-7-1A (hp)	10%	151 $\pm$ 24	3.47	4.50	.115
SG-7-1B (hp)	10%	149 $\pm$ 24	3.22	4.47	.106
SG-7-2A (s)	20%	141 $\pm$ 23	5.48	4.67	.196
SG-7-3B (hp)	30%	151 $\pm$ 28	7.70	5.28	.298

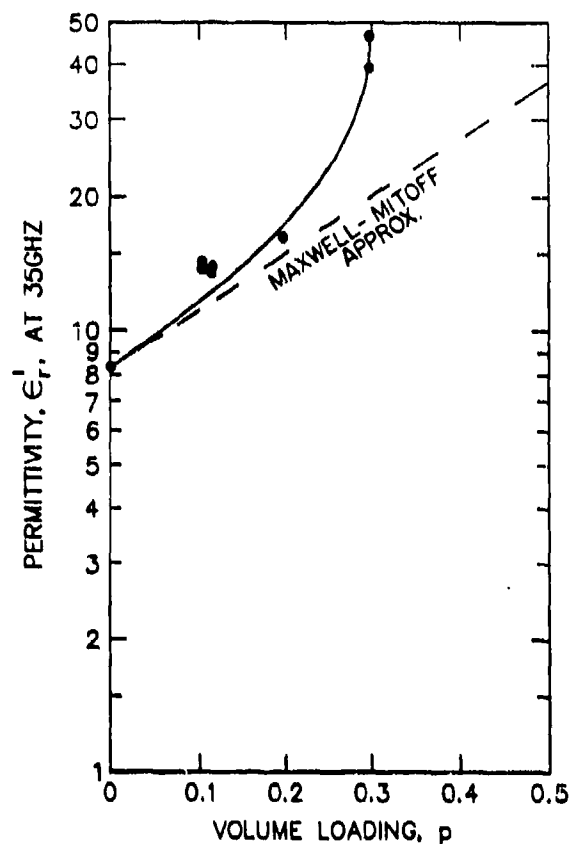
## Notes:

hp = processing by hot pressing around 600 °C and 300 psi.

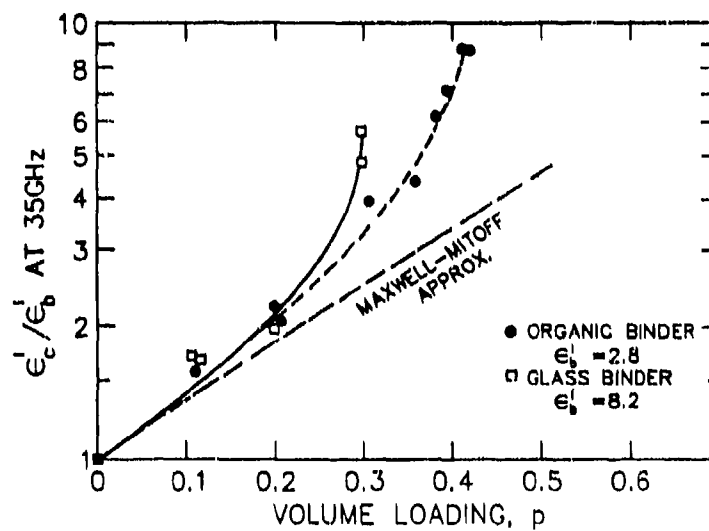
s = processing by sintering only at 535 °C for 20 min.

Sample 2B broke during machining.

Sample 3A exhibited gross conductivity.



14. Relative permittivity,  $\epsilon'_r$ , vs. volume loading,  $p$ , for  $\text{Ni}_{12}\text{Cr}_8$  alloy,  $10\text{ }\mu\text{m} < d < 20\text{ }\mu\text{m}$ , in lead-solder glass binder, measured at 35 GHz.



15. Scaled comparison of permittivity behavior,  $\epsilon'_c/\epsilon'_b$ , at 35 GHz, for artificial dielectrics with two different binders.  $\text{Ni}_{12}\text{Cr}_8$  particles in polyurethane [ $\epsilon'_b = 2.8$ ] and in lead-solder glass [ $\epsilon'_b = 8.2$ ].

imaginary parts of the permeability. The bars on the experimental represent the full spread of several data points obtained from various disks of the same nominal (or identical) loadings. The agreement is fully satisfactory, a tribute to the quality of the measurement method and to the adequacy of the model.

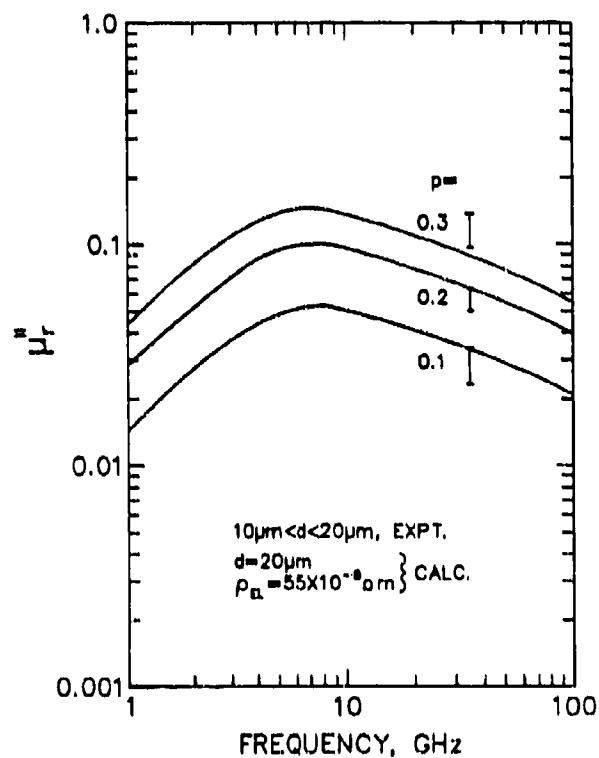
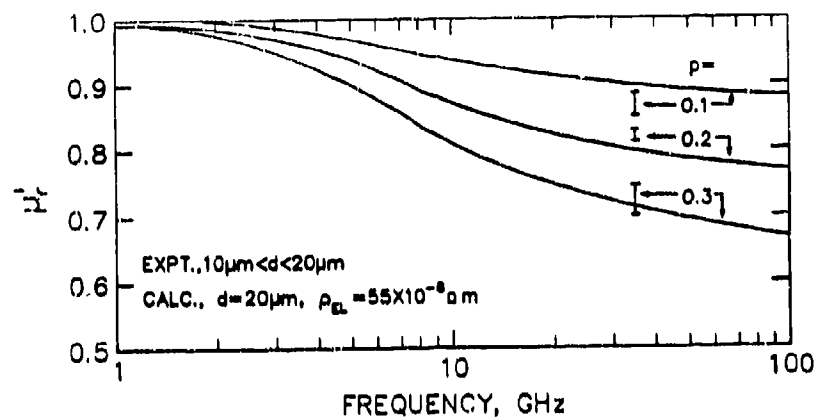
#### IV. IMPROVED MODELING OF RANDOMLY PACKED ARTIFICIAL DIELECTRICS

The idea of a model dielectric which consists of an assembly of metallic globules separated from each other by insulating material (= an artificial dielectric) goes back at least as far as Faraday in 1837. It represents one limit in the properties of inhomogeneous media (or composite materials) which have provided problems for theorists and engineers for the ensuing century and half. An excellent survey of the early history and of the evolution of seminal concepts has been recorded by Landauer [6]. Indeed the subject remains one of active interest, as witnessed by several recent topical conferences [7,8]. It is also relevant to note that for composite materials the calculation of dielectric constant, magnetic permeability, electrical conductivity, thermal conductivity and diffusion properties can often be formulated in precisely analogous ways. Thus there is a common literature for such phenomena from which one can readily apply theoretical and experimental results to the various properties. While we cited a number of papers of special interest to us in Reference 2, particularly with regard to periodic arrays, it may be helpful to the reader to know of other references of the post-war decades. The selection is not intended to be complete in any way, but represents some papers which either come well recommended or upon which we stumbled en route [9-15]. These give some idea of the range of publication media and also would serve to help one find other work on the subject.

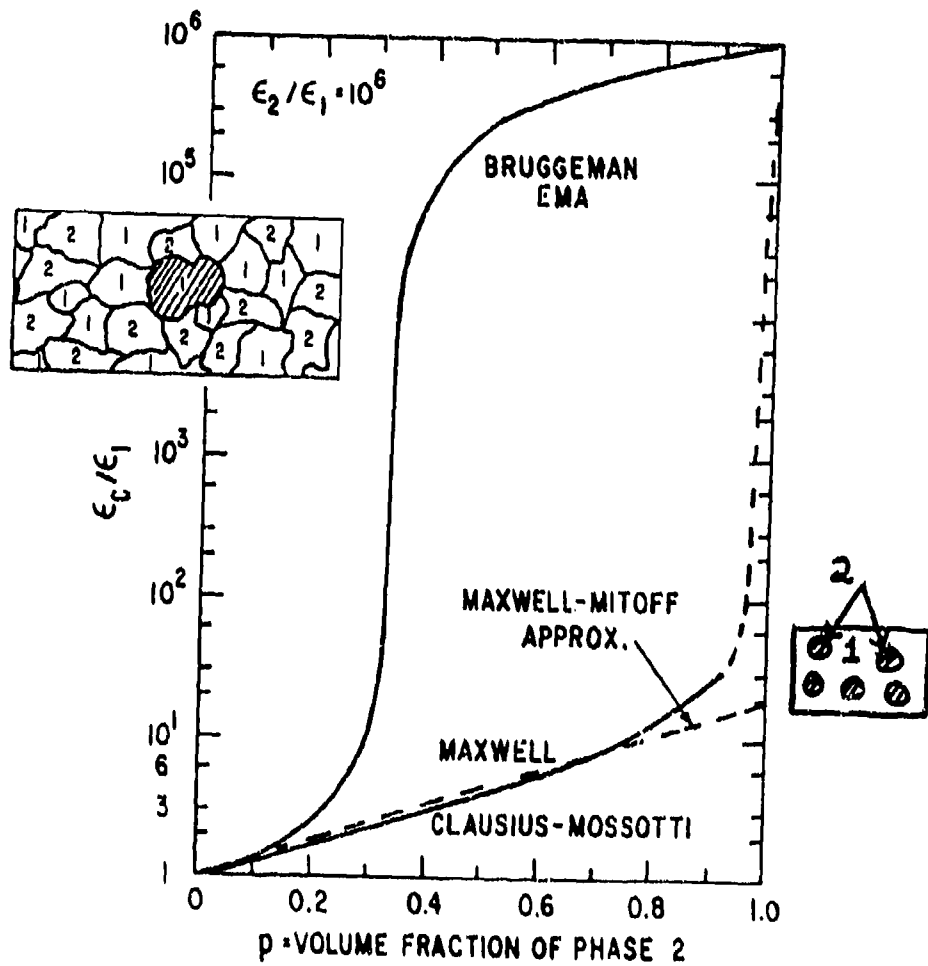
There is a basic distinction between several classes of models of heterogeneous dielectric media. More modern theory follows the work of Bruggeman [6,16]. This is a symmetrical (two-component) effective medium model wherein particles of type 1 are mixed randomly in some proportion with those of type 2, so that each may be surrounded by particles of both types. If one type is conducting and the other insulating, there will be a percolation threshold composition at which conducting paths are established. The volume loading for this to occur is about 0.15 to 0.2. This model is often labeled EMA (eff.med.approx.). The upper inset in Figure 17 depicts this topology and the curve shows the dramatic change that occurs at percolation according to one mathematical model.

In another (older) class of model one assumes that particles of type 1 are completely surrounded by material of type 2. It is clearly necessary to specify whether metal has been added to a dielectric host or vice versa, i.e., the model is unsymmetrical. This class of model is associated with the names of Maxwell, Maxwell-Garnett, Clausius and Mossotti, and Lorentz and Lorenz. It too is really an effective medium (or molecular field) model. It is variously called by any of the names just cited, e.g., MGT, CM, etc. Real-life examples of this model are ordered (cubical) arrays of spheres in a different medium, or an otherwise correlated medium such as coated spheres in a random arrangement, with each metal particle surrounded by a concentric dielectric coating. The lower right inset in Figure 17 describes this model and the curve for its behavior is indicated. Our coated alloy particles fall into this class of composites.

In recent years, rigorous calculations (and some measurements) of the ordered arrays have appeared and they have relevance for the random coated array. Features of these theories are the significant effects of higher order multipoles beyond the dipole-dipole model and the (obvious, but sometimes ignored) maximum packing limits. These factors, along with departures from metal particle sphericity usually promote upward deviations in the curve of  $\epsilon'$  vs.  $p$ . Nevertheless, the existing theoretical models fall short of describing the effects reasonably quantitatively.



16. Comparison of experiment and model calculations:  $\mu_r'$  and  $\mu_r''$  vs. frequency, various loadings; for  $\text{Ni}_{52}\text{Cr}_8$  alloy powder,  $10\mu\text{m} < d < 20\mu\text{m}$ , in lead-solder glass. Data at 35 GHz only, from GE-RSO (J. Hanson).



17. Comparison of classical dielectric models of percolating (Bruggeman) versus non-percolating (Maxwell/Clausius-Mossotti) systems.



In discussion with our consultant, W.T. Doyle of Dartmouth, who had carried out complete multipole calculations for ordered arrays of conducting spheres [17], we conceived of an instructive but very much simplified approach to the problem of randomly packed artificial dielectrics. The germ of the idea comes from inspection of a micrograph of one of our actual composites of Ni-Cr particles in polymer at 10% volume loading (from Figure 4a of Reference 3), in comparison with a schematic diagram used by microscopist-ceramists to estimate porosity. These are shown in Figure 18. In a limited, but incorrect, sense the schematic diagram may be termed an "idealized random" composite with the volume loading as indicated. While there is no periodicity, it lacks the density fluctuations of a truly random loading. On the positive or idealized side, the particles (= dots) never touch or coalesce until the packing limit is reached! This would be about 63% for a 3-D random array. Thus this "random" schematic actually represents a *correlated* medium. In fact such an assumption of a correlated medium was included [18] in the "estimated calculation" for a random or disordered array carried out by the Australian group [9] by using scaling arguments on the rigorous results for an ordered array.

In contrast, when one examines the micrograph of the actual composite, local clustering is quite evident. This comparison led us to consider a model based on pair interactions. Prof. Doyle's report on this model, performed as a subcontract follows.

#### IV.1 Pair Interactions in Artificial Dielectric Media (W.T. Doyle)

##### IV.1.1 Introduction

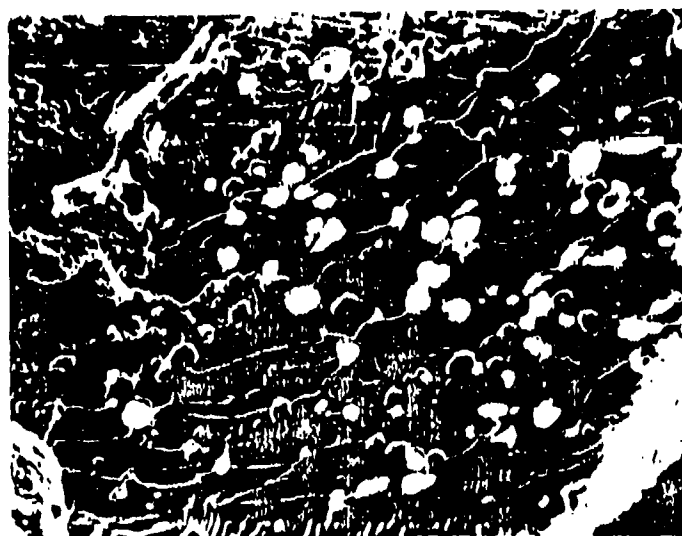
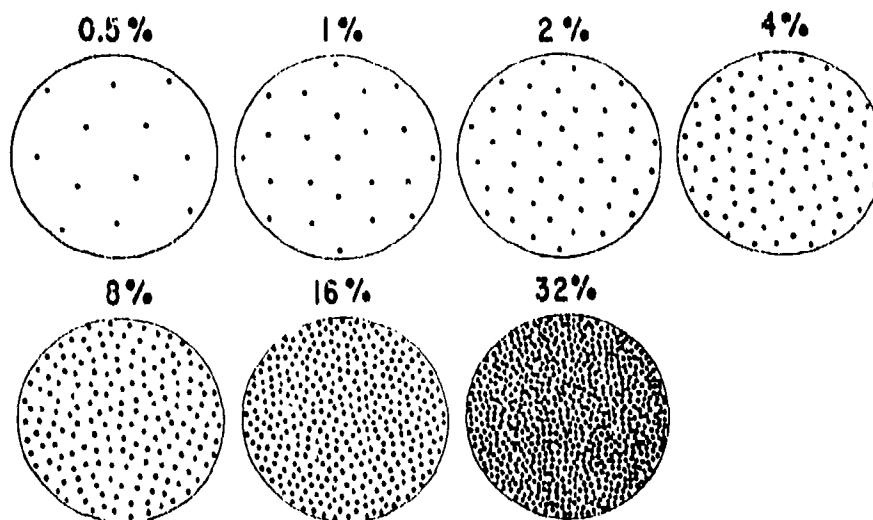
The average permittivity of an inhomogeneous medium composed of spheres of one substance embedded in a continuum of a different material (cermet topology) is, in general, a complicated function of the permittivities of the constituents, the volume filling factor, particle shape and size, and the details of the particle distribution function. Although the permittivities may be complex and depend upon frequency, we shall be concerned only with perfectly conducting particles in the electrostatic limit.

In the simplest case of a regular array of spheres of uniform size the permittivity may be computed exactly [17, 19, 20]. When one or the other of the various parameters has a non-zero variance, the problem becomes substantially more difficult. If all parameters exhibit wide variances the problem is essentially intractable. Fortunately, in practice, it is possible to obtain nearly mono-disperse distributions of good spheres. However, even an array of uniform sized spheres presents difficulties when the spheres are randomly distributed in space. For such media the permittivity may be calculated only approximately.

If only dipole interactions are present, the permittivity of an isotropic medium is given by the well-known Clausius-Mossotti relation. For regular arrays this case occurs in the limit of low filling factors. For random distributions close encounters can occur even with low filling factors, and corrections may be necessary even with low particle densities. Experiments with nominally "random" media often exhibit substantial departures from the predictions of the approximate formulas, usually of the kinds to be expected from enhanced particle interactions due to particle clustering.

##### IV.1.2 Clustering Effects

In a neutral dielectric medium only dipole and higher multipolar interactions exist, and all depend inversely upon increasing powers of the distance between the particles of the medium. As a consequence, the multipole interactions grow rapidly with increasing volume filling factor. Because



18. Comparison of an actual composite: Ni-Cr/polyurethane,  $p=0.1$ ,  $20\text{ }\mu\text{m} < d < 37\text{ }\mu\text{m}$ , SEM of cold-microtomed sample; with an "idealized random" composite schematic used by microscopists to estimate porosity.

they are positive, all multipole contributions lead to an increase in the dielectric constant with decreasing interparticle distance. A macroscopic manifestation of this is a strong non-linearity of the dielectric constant when plotted as a function of volume filling factor. All experiments and physically valid theoretical approximations show this nonlinear behavior. An immediate consequence of this simple arithmetic fact is that any departure from strict constancy of the density of the medium leads to an enhancement of the dielectric constant.

Density fluctuations are inescapable in a random medium. They occur statistically, if for no other reason, although there are often stronger variances associated with fabrication, such as incomplete stirring, particle cohesion, settling, substrate distortion, interparticle forces, and other factors. Any or all of these density fluctuations can be expected in any given sample, and all can lead to an increase in the measured macroscopic average dielectric constant. We shall refer to all such enhancements as "cluster effects."

The problems associated with an unrestricted density variation are formidable, if not actually unsolvable. In this report we shall examine one of the simplest types of clustering effect: the permittivity enhancement produced by the presence of a population of close *pairs* of particles in a medium consisting of perfectly conducting monodisperse spheres. We shall only consider interactions between isolated pairs of particles. All larger clusters of particles and larger scale density fluctuations will be ignored.

The interaction of an isolated pair will be treated exactly, including the effect of all higher multipoles mutually induced by the partners on each other. As will be seen, the pair interaction leads to an enhancement of the effective polarizability of the pair. Once the pair polarizability has been found, the pair may be treated as a molecular dipole in calculating the dielectric constant of an ensemble of mixed isolated particles and pairs.

#### IV.13 Pair Polarizabilities

Laplace's equation is separable in bispherical coordinates, so the problem of two conducting spheres in a uniform external field may be solved exactly. Using this coordinate system Levine and McQuarrie [21] obtained series expressions for the total polarizability of a system of two spheres with arbitrary separation. We follow their treatment here.

The polarizability of the pair may be written

$$\alpha_{pair} = \alpha_1 + \alpha_2 + \alpha_{12} \quad (1)$$

where  $\alpha_1 = \alpha_2 = R^3$  is the polarizability of either of the two identical isolated spheres, and  $\alpha_{12}$  is the incremental polarizability caused by each sphere's *total* field on the other. Since the solution is exact, this enhanced polarization includes the effect of *all* higher multipoles induced on these two spheres in a *uniform* external field.

The polarizability tensor of a pair is axially symmetric so there are two independent components  $\alpha_{12,L}$  and  $\alpha_{12,T}$ , longitudinal and transverse to the pair axis, respectively. The average polarizability of an ensemble of pairs with axes distributed isotropically is given by

$$\alpha_{12,0} = (\alpha_{12,L} + 2\alpha_{12,T})/3 \quad (2)$$

For an isotropic random medium  $\alpha_{12,0}$  is the important quantity.

The polarizabilities  $\alpha_{12,T}$  and  $\alpha_{12,L}$  are given by

$$\alpha_{12,T} = 2R^3 \sinh^3 \eta_0 \sum_{s=2}^{\infty} (-1)^{s-1} (\sinh s \eta_0)^{-3} \quad (3)$$

and

$$\alpha_{12,L} = 4R^3 \sinh^3 \eta_0 [(S_0(\eta_0)S_2(\eta_0) - S_1(\eta_0)S_1(\eta_0))/S_0(\eta_0)] - 2R^3 \quad (4)$$

where  $\eta_0$  is defined by

$$\cosh \eta_0 = \frac{r}{2R} = x \quad (5)$$

The pair separation parameter  $x = r/2R$  is determined by the interparticle center-to-center distance,  $r$ , and the sphere radius,  $R$ . The functions  $S_0(\eta_0)$ ,  $S_1(\eta_0)$ , and  $S_2(\eta_0)$  are given by

$$S_k(\eta_0) = \sum_{l=0}^{\infty} \frac{(2l+1)^k}{\exp[(2l+1)\eta_0] - 1} \quad (6)$$

The polarizabilities obtained with equations (2)-(4) (normalized to  $R^3$ ) are tabulated in Table 2 and shown graphically in Figure 19. From the figure it is clear that a substantial enhancement of the dielectric constant can occur in the presence of many closely spaced pairs. For spheres in contact, all of the incremental polarizabilities are of the same order of magnitude as the polarizability of an isolated sphere. The average polarizability,  $\alpha_{12,0}$ , which determines the dielectric constant of a random distribution, drops off very rapidly with increasing separation of the spheres in a pair.

#### IV.1.4. Dielectric Constant

The values given in Table 2 are for pairs of particles. The incremental polarizabilities *per particle* are half as large as the tabulated values. To find the average effective polarizability of a particle of the medium we must add one half of the incremental polarizability for a given pair,  $\alpha_{12,0}(x)/2$ , with separation parameter  $x$ , to the isolated sphere polarizability,  $R^3$ , and then average over all pairs in the medium. Thus

$$\langle \alpha \rangle = R^3 + 1/2 \int n_2(x) \alpha_{12,0} dx \quad (7)$$

where  $n_2 = N_2/N$  is the fraction of particles that are members of pairs,  $x$  is the interparticle distance parameter, and  $R$  is the particle radius.

Equation (7) shows that we need further information about the particle distribution in order to calculate the effective polarizability. This kind of detailed structural knowledge is required with any approximation higher than the dipole approximation. In the present case we must know, or make some assumption about, the number of pairs present for each value of the separation parameter  $x = r/2R$ .

The simplest assumption we can make regarding  $n_2(x)$  is that all of the pairs have the same separation,  $\bar{x}$ , say. Then we have

$$\langle \alpha \rangle = R^3 (1 + n_2(\bar{x}) \alpha_{12,0}(\bar{x}) / 2R^3) \quad (8)$$

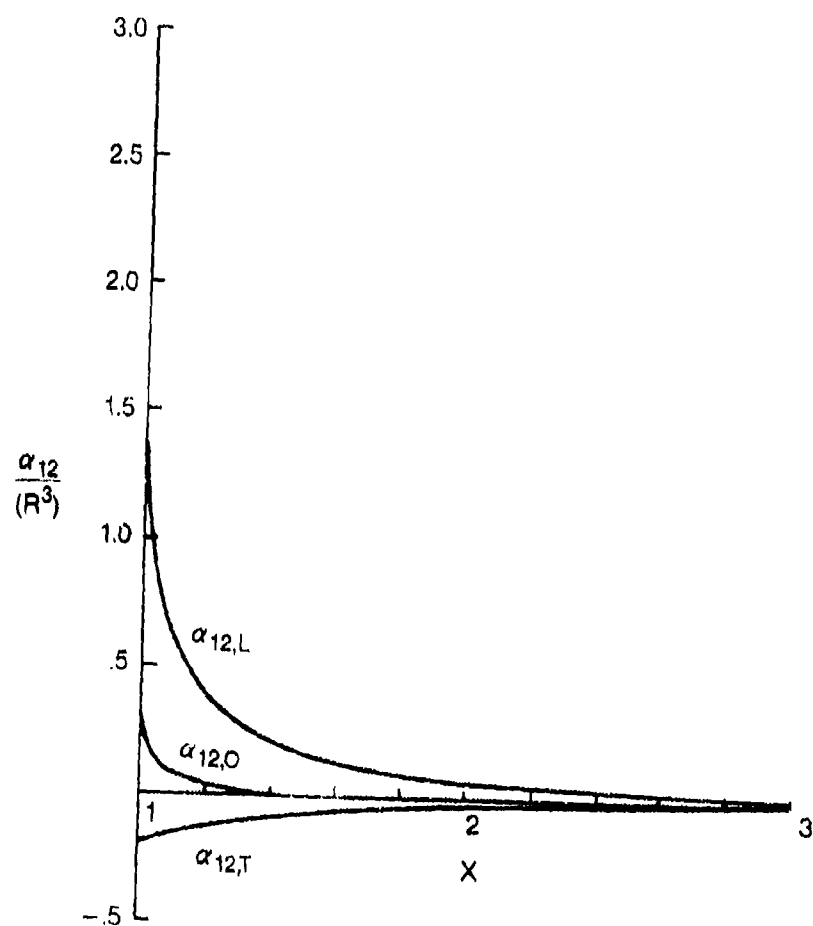
so that there are only two adjustable parameters; the fractional number of particles in pairs,  $n_2(\bar{x})$ , with the effective separation parameter  $\bar{x}$ . The value of  $\alpha_{12,0}(\bar{x})$  is taken from Table 2, using the

TABLE 2

Incremental Polarizabilities  $\alpha_{12}$ , Per Pair (Normalized to  $R^3$ )  
as a Function of the Separation Parameter,  $x=r/2R$ .

Subscripts T, L, and O designate the transverse, longitudinal  
and average composites, respectively. (Sphere radius is  $R$ , and  
interparticle separation, center-to-center, is  $r$ .)

$x$	$\alpha_{12,T}$	$\alpha_{12,L}$	$\alpha_{12,O}$
5.00000	-0.0020	0.0040	0.0000
4.00000	-0.0039	0.0078	0.0000
3.00000	-0.0092	0.0187	0.0001
2.00000	-0.0307	0.0648	0.0012
1.90000	-0.0356	0.0762	0.0016
1.80000	-0.0417	0.0904	0.0023
1.70000	-0.0492	0.1086	0.0034
1.60000	-0.0586	0.1323	0.0050
1.50000	-0.0704	0.1641	0.0078
1.40000	-0.0853	0.2083	0.0126
1.30000	-0.1043	0.2729	0.0215
1.20000	-0.1285	0.3757	0.0396
1.10000	-0.1591	0.5695	0.0838
1.09000	-0.1625	0.5998	0.0916
1.08000	-0.1660	0.6336	0.1005
1.07000	-0.1696	0.6719	0.1109
1.06000	-0.1733	0.7159	0.1231
1.05000	-0.1770	0.7673	0.1377
1.04000	-0.1809	0.8291	0.1558
1.03000	-0.1848	0.9066	0.1790
1.02000	-0.1887	1.0107	0.2111
1.01000	-0.1928	1.1730	0.2625
1.00900	-0.1932	1.1959	0.2698
1.00800	-0.1936	1.2210	0.2779
1.00700	-0.1940	1.2487	0.2869
1.00600	-0.1944	1.2797	0.2970
1.00500	-0.1948	1.3152	0.3085
1.00400	-0.1953	1.3569	0.3221
1.00300	-0.1957	1.4078	0.3388
1.00200	-0.1961	1.4746	0.3608
1.00100	-0.1965	1.5766	0.3945
1.00090	-0.1965	1.5908	0.3992
1.00080	-0.1966	1.6064	0.4044
1.00070	-0.1966	1.6236	0.4101
1.00060	-0.1967	1.6429	0.4165
1.00050	-0.1967	1.6650	0.4239
1.00040	-0.1967	1.6910	0.4325
1.00030	-0.1968	1.7229	0.4431
1.00020	-0.1968	1.7649	0.4571
1.00010	-0.1969	1.8299	0.4787
1.00009	-0.1969	1.8391	0.4818
1.00008	-0.1969	1.8492	0.4851
1.00007	-0.1969	1.8604	0.4889
1.00006	-0.1969	1.8730	0.4931
1.00005	-0.1969	1.8874	0.4979
1.00004	-0.1969	1.9046	0.5036
1.00003	-0.1969	1.9257	0.5106
1.00002	-0.1969	1.9540	0.5200
1.00001	-0.1969	1.9983	0.5348
1.00000	-0.1969	2.8082	0.8048



19. Incremental polarizabilities,  $\alpha_{12}$ , (normalized to  $R^3$ ) versus separation parameter  $x = r/2R$ .

appropriate average particle separation parameter  $\bar{x}$ .

The effective polarizability is then used in the dipole approximation for the dielectric constant. The Clausius-Mossotti expression

$$\epsilon = \epsilon_0 \left( 1 + \frac{4\pi N \langle \alpha \rangle}{1 - \frac{4}{3}\pi N \langle \alpha \rangle} \right) \quad (9)$$

is consistent with our assumption that only pairs and isolated spheres are present.

#### IV.1.5. Comparison with Experiment

Our results apply to a suspension of conducting spheres in the long wavelength (electrostatic) limit with intermediate filling factors. Although the Clausius-Mossotti expression for isolated spheres is independent of the sphere size, the pair calculations assumed equal-sized spheres, so we should restrict our comparison to fairly mono-disperse samples. Some of the older literature reviewed by DeLoor [10] report dielectric constant enhancements that can be attributed to cluster effects. The measurements of Guillien [22] on emulsions of Hg in oil are of particular interest, because both particles and host are liquids so the particles are exceptionally smooth and spherical. We shall compare our calculations with Guillien's low frequency results and with the recent microwave measurements reported in the technical reports of this contract [2,3].

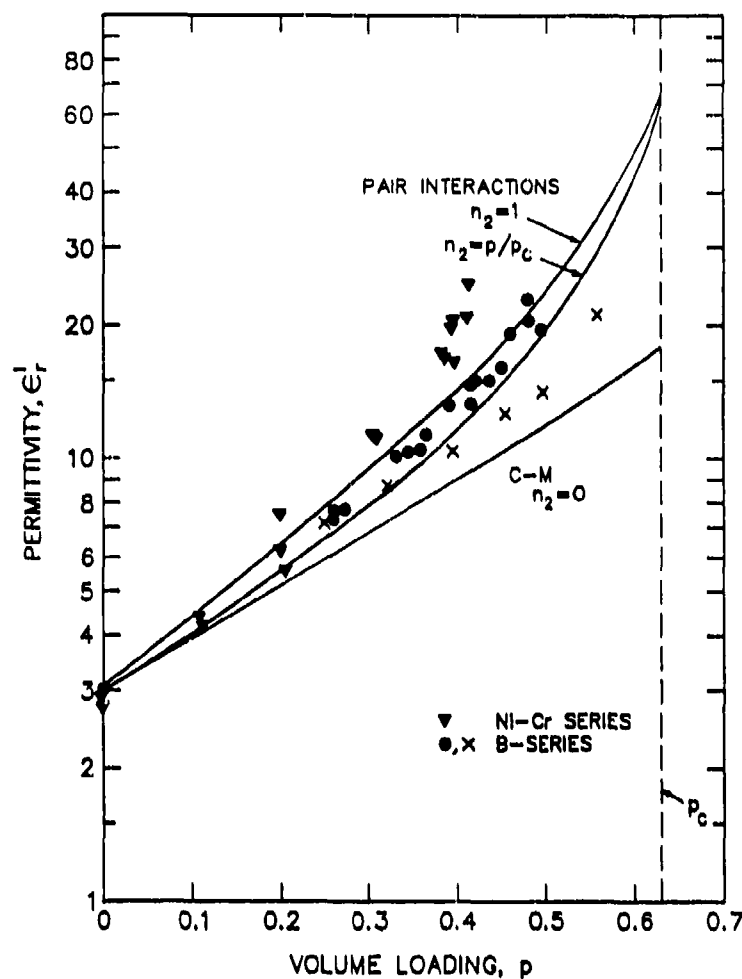
The largest possible isotropic dielectric constant enhancement obtainable with *isolated* pairs occurs when all of the spheres form pairs in contact. The number of isolated spheres is then zero and the number of pairs is maximum, provided that no sphere is permitted more than a single point of contact. From Table 2 we see that at contact, the average polarizability per sphere is equal to  $1.4024R^3$ . The solid lines in Figures 20 and 21 show the Clausius-Mossotti results, with and without pairing. The bottom curve is the Clausius-Mossotti result, with no pairs present. The upper two curves show the pair-enhanced dielectric constant according to two extreme assumptions about the dependence of the pairing probability upon particle density, as discussed next.

In the topmost curves of Figures 20 and 21 we assume that the pairing probability is independent of particle density. One conspicuous consequence of this assumption is that the derivative of the curve of dielectric constant versus filling factor is larger than the Clausius-Mossotti value  $3\epsilon_0$  at  $p = 0$ . This is admittedly an extreme assumption, in that complete pairing is assumed even in the limit of very small filling factor. Such a high clustering tendency may be appropriate for cohering particles that resist breakup by stirring. Some of the experimental data seem to involve some low density clustering. Whether or not such media exist, the example serves to show that even clusters as small as pairs can produce significant effects.

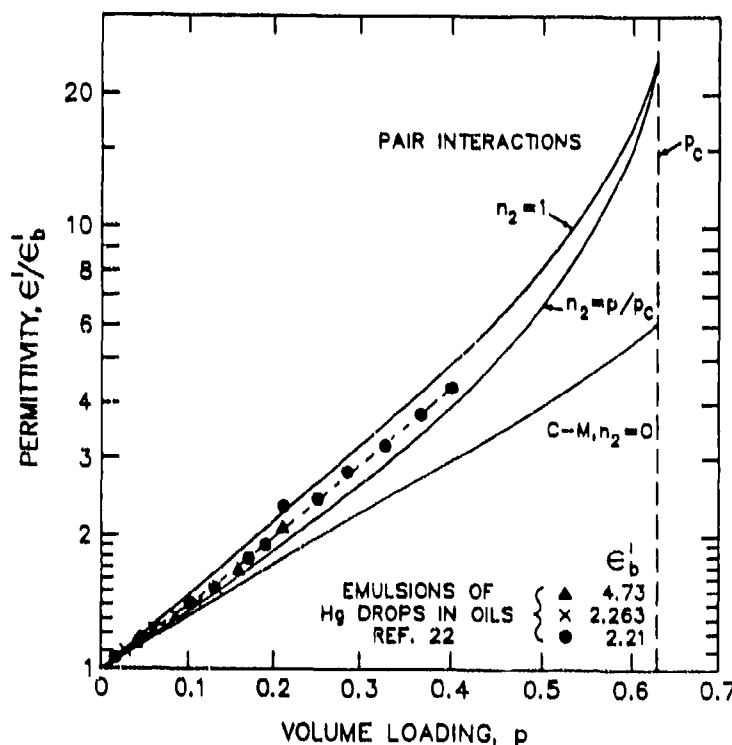
Another simple case is obtained by assuming that the pair density is simply proportional to the filling factor  $p$ . Assuming that  $n_2(x) = p/p_c$ , we have

$$\langle \alpha \rangle = R^3(1 + \alpha_{12,0}(1)p/2p_cR^3) \quad (10)$$

Setting  $p_c = 0.63$ , the value appropriate for a random medium, we get the middle curves in Figures 20 and 21. This is a more natural assumption for non-cohering particles, since for such materials one would expect the pair density to go to zero in the limit of low filling factors. With this assumption there are no pairs present at zero filling factor, so the initial slope is equal to  $3\epsilon_0$  in agreement with



20. Dielectric constant,  $\epsilon'$ , vs. volume loading,  $p$ . Calculated models with and without pairing,  $n_2$ . Experimental data from Reference 3, Figures 5 and 7.



21. Reduced permittivity,  $\epsilon'/\epsilon_b$ , versus volume loading,  $p$ . Calculations as for Figure 20. Data for spherical drops of Hg in heavy oil, from Reference 22.



the Clausius-Mossotti result.

The calculated curves are the same in Figures 20 and 21 except for normalization. The points shown are the experimental results. Figure 20 shows microwave measurements on solid particles from Reference 3, Figure 5 and 7. Microscopic examination showed the samples to be relatively mono-disperse distributions of nearly spherical particles. Figure 21 shows Guillien's measurements on Hg emulsions in oil [22]. The similarity of the experimentally measured dielectric enhancements of the solid samples in Figure 20 and the liquid sample in Figure 21 is worth noting, since the liquid sample presumably exhibits an enhancement produced by density variation alone, uninfluenced by a distribution of particle shape. The large enhancements exhibited by some of the solid samples in Figure 20 could be due either to a distribution of particle shape and/or larger scale density variations.

#### IV.1.6 Conclusions

Using the polarizabilities in Table 2, together with equations (7) and (9), one could easily calculate the dielectric constant in the presence of an arbitrary distribution of pair densities. However, calculations based on detailed assumptions regarding the pair distribution would require a correspondingly detailed microscopic sample characterization.

In the absence of a detailed sample characterization, we can estimate the magnitude of the pair contributions to dielectric enhancement by assuming that all of the pairs have the same (average) separation parameter. Then only the product of the pair density and the incremental polarizability enters the generalized Clausius-Mossotti relation (9) via equation (8). In general, a range of densities and incremental polarizabilities yield the same enhancement.

Isolated particle pairs can give rise to a substantial enhancement of the long wavelength dielectric constant of a medium of metal spheres. Large enhancements require large numbers of close pairs. For spheres in contact, the incremental polarizability is of the same order of magnitude as that of a single isolated particle. Whatever the actual pair distribution, only very close pairs make a significant contribution to dielectric constant enhancement.

#### IV.2 Further Experimental Comparisons with Theoretical Models

In the preceding section we have seen that pair interactions alone can produce permittivity enhancements (above the Clausius-Mossotti values) as large as those often observed in random metal-particle composites. The example shown in Figure 21 is striking because of the ideal materials of that experiment [22], i.e., both phases liquid and perfect sphericity guaranteed for the metal particles. It would be foolish to put heavy weight on one or the other of the two limiting calculated models, inasmuch as the assumption of isolated pairs quickly breaks down with increasing packing. The apparent trend toward convergence between experiment and model is success enough in an otherwise almost intractable problem. For recent examples of the difficulty in treating the theoretical problem with rigor, see Reference 15.

Subsequent to Doyle's report we encountered another ideal experiment, in the chemical engineering literature on electrical conductance [23]. Beds of solid resin spheres (0.2 to 1.0 mm diameter) were fluidized by aqueous solutions of sodium chloride. By varying resin material as well as saline concentration, a wide range of intrinsic conductivity ratios could be attained. Volume fractions ranging from as low as 0.04 to as high as 0.6 were achieved. Conductivity measurements were carried out at 1.6 kHz using specially prepared electrodes in the fluidized bed. Turner's work provides a nice overlap as well as an extension of the range studied by Guillien [22].

In Figure 22 we show the superposition of the reduced permittivity and reduced conductance data in comparison with several model calculations. First one should observe the rather smooth overlap between the two sets of experiments. Together these data sets provide an empirical reference solution to the problem of an artificial dielectric composed of non-percolating ("coated") randomly-arrayed, reasonably-monodisperse spheres. Secondly, we note again how well the oversimplified pair interaction model ( $n_2 = p/p_c$ ), comes close to describing these experimental observations. This is in strong contrast to the quasi-empirical, quasi-theoretical model of McKenzie et al. [19] which accounted for higher order multipoles but was keyed by scaling to the packing limit at  $p_c = 0.63$ . The base reference curve, the dipolar-only model of Maxwell and Clausius-Mossotti is also shown. Our delight with this modeling success led us to describe it at an APS meeting [24].

Finally, in Figure 23 we return to the microwave frequency experiments with solid metal spheres, repeated in simplified schematic from Figure 20. The ensemble of data points for each of the two metal alloy systems has been replaced by an average data line. [The data from the B-series of alloy powder are broken into one line and an outlying set of x-points which deviate for reasons not yet understood.] We are struck by the relative positions of the B-series line and the Doyle pair-interaction model when viewed together with Figure 22. Thus most of the B-series data resemble the behavior of the ideal sphere experiments. It should be recalled (as in Section III.1 and Figure 15, herein) that the Ni-Cr alloy powder suffered somewhat from non-spherical deviations. Thus we arrive at approximate experimental convergence of permittivity behaviors with deviations understood in many cases.

Overall, the progress on both the experimental and the modeling (or "theoretical") aspects of these systems is quite satisfying. Reasonably good analytic/empirical tools are in hand with which to predict the permittivity of random metal-particle artificial dielectrics over a wide range of frequencies up to and including the millimeter wavelength range.

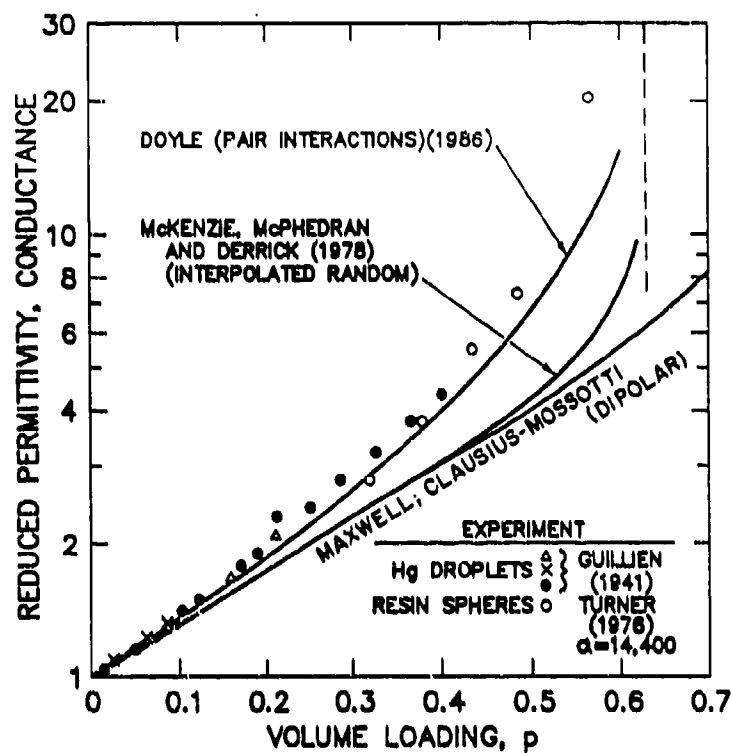
## V. CONCLUSIONS

In this report period we have completed the tasks set forth in the contract work statement, dealing with the essentially non-magnetic artificial-dielectric composites.

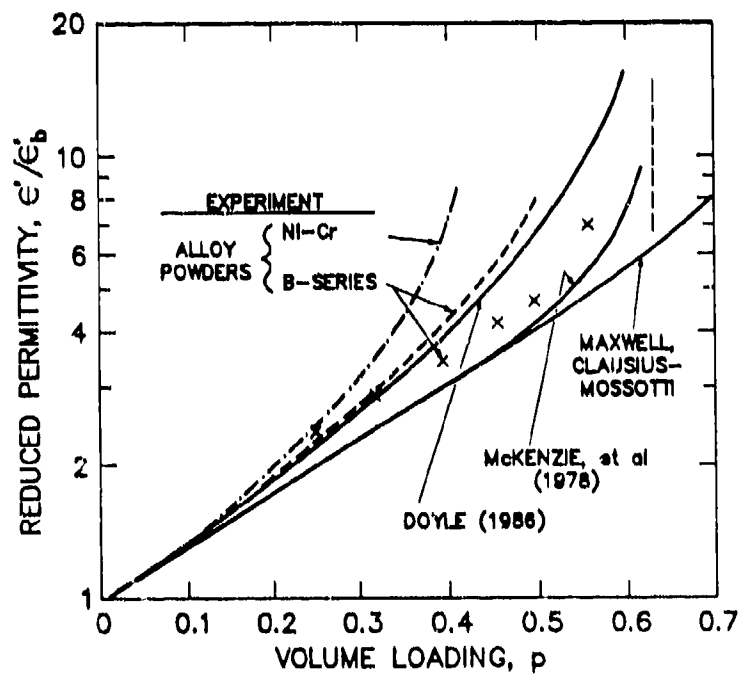
We have been able to improve the electromagnetic evaluation of polymeric binder composites in the centimeter wavelength range, 2-18 GHz, mainly through collaboration with staff scientists at the Naval Research Laboratory. The earlier stage foray [3] into the millimeter wavelength range, at 35 GHz, (with a colleague at GE-Philadelphia) has now been complemented on several polymeric composite samples both into the  $K_a$ -band (26-40 GHz) and the W-band (75-110 GHz) working at NRL.

The results support our earlier suggestion that the permittivity values change but little over the full range covered. On the other hand, the induced permeability results are reasonably consistent with the behaviors calculated in our first report [2]. This success provides a firm foundation for extending these concepts to the more difficult metallic magneto-dielectrics discussed in the classified reports under this contract.

The main interests in the permittivity results have focussed on their dependence on volume loading and their scaling properties with change of binder. Reasonably extensive results on the polymeric binder composites show very good agreement between 10 GHz data and 35 GHz data; both depart smoothly from the host binder value and exhibit substantial upward deviation from the classical Clausius-Mossotti dipolar model. Experiments with an alternative inorganic (glassy) binder show qualitatively similar behavior (measured at 35 GHz) along with higher values for the dielectric



22. Reduced permittivity or conductance data from several ideal experiments (References 22 and 23) compared with several multipole models and the classical dipole model.



23. Calculated model behaviors of permittivity versus volume loading (as in Figure 22), compared with averaged data from microwave experiments on solid metal powders from this work.

constants. When adjusted for binder permittivity, the variation of  $\epsilon'_c/\epsilon'_b$  for the two binder systems is in very good agreement out to  $p \sim 0.2$ , but deviates at higher loadings, probably because of powder particle distortion in the inorganic composite preparation. These same composites showed induced complex permeability results in excellent agreement with the model calculations [2].

We have also been successful in improving the modeling of permittivity behavior of randomly packed artificial dielectrics. This has been a two-faceted success, i.e., on the empirical and on the "theoretical" fronts. The empirical success rests on the discovery in the literature of several rather different sets of results from ideal experiments involving truly spherical second phase particles, well randomized, and non-percolating [22,23]. Some of our own data sets strongly resemble this "ideal behavior." On the "theoretical" side, we have developed, through the work of our consultant, Prof. Doyle, a rather simple pair-interaction model which is a naive oversimplification in part but serves to show the importance of local clustering and higher-order multipole effects [24]. The pair-interaction model comes closer to describing the experimental results than any other model known to us. This convergence, even if it is not to be taken very seriously, gives one a feeling of confidence and predictive control in considering the dielectric behavior. We note in passing that this approach should also be applicable to the real part of the permeability in the magneto-static limit, and will be examined in Part B of this report.

## REFERENCES

- [1] I.S. Jacobs, H. Kirtchik, J.M. McGrath and R.N. Silz, "Magnetic RAM Technology - Phase II (U)," AFWAL-TR-82-1040, Final Technical Report for Contract F33615-80-C-1040, General Electric Company, Sept. 1982, SECRET.
- [2] I.S. Jacobs, "Advanced Artificial Dielectric Materials for Millimeter Wavelength Applications," Annual Technical Report for Contract No. N00014-83-C-0447, Period 1 Aug. 83 to 30 Sept. 1984, General Electric CRD, Oct. 1984.
- [3] I.S. Jacobs, "Advanced Artificial Dielectric Materials for Millimeter Wavelength Applications," Annual Technical Report, Part A, for Contract No. N00014-83-0447, Period 1 Oct. 1984 to 30 Sept. 1985, General Electric CRD, Dec. 1985, (85-SRD-030).
- [4] I.S. Jacobs, S.A. Miller, H.J. Patchen, J.O. Hanson, F.J. Rachford and S. Browning, "Electromagnetic Properties of Non-Percolating Random Metal-Particle Composites," *Bull. Am. Phys. Soc.* 31, 667 (1986).
- [5] S.P. Mitoff, "Properties Calculations for Heterogeneous Systems" in *Advances in Materials Research*, H. Herman, ed. (Interscience, John Wiley, New York, 1968) vol. 3, pp 305-329.
- [6] R. Landauer, "Electrical Conductivity in Inhomogeneous Media," in *Electrical Transport and Optical Properties of Inhomogeneous Media*, edited by J.C. Garland and D.B. Tanner, AIP Conference Proceedings, No. 40, (American Institute of Physics, New York, 1978) pp. 2-45.
- [7] See the whole *Proceedings* issue of Reference 6.
- [8] *Physics and Chemistry of Porous Media*, edited by D.L. Johnson and P.N. Sen, AIP Conference Proceedings, No. 107 (American Institute of Physics, New York, 1984).
- [9] D. Polder and J.H. Van Santen, "The Effective Permeability of Mixtures of Solids," *Physica*, 12, 257-271 (1946).
- [10] G.P. deLoor, "Dielectric Properties of Heterogeneous Mixtures," Thesis, University of Leiden, 1956.
- [11] J.A. Reynolds and J.M. Hough, "Formulae for Dielectric Constant of Mixtures," *Proc. Phys. Soc. (London)*, 70B, 769-775 (1957).
- [12] L.S. Taylor, "Dielectric Properties of Mixtures," *IEEE Trans. Ant. Propag.* AP-13, 943-947 (1965).
- [13] L.K.H. van Beek, "Dielectric Behavior of Heterogeneous Systems" in *Progress in Dielectrics*, vol. 7, pp 70-114, (1967).
- [14] P.C. Waterman and N.E. Pedersen, "Electromagnetic Scattering by Periodic Arrays of Particles," *J. Appl. Phys.* 59, 2609-2618 (1986). This paper is noteworthy in a negative sense for the statement "Random arrays are considered briefly, and we note that in the low-frequency limiting cases higher multipole contributions drop out, so that only dipole contributions are important." Our results and interpretation are completely opposite.
- [15] F. Lado and S. Torquato, "Effective properties of two-phase disordered composite media. I. Simplification of bounds on the conductivity and bulk modulus of dispersions of impenetrable spheres," *Phys. Rev. B* 33, 3370-3378 (1986); S. Torquato and F. Lado, "Effective properties of

two-phase disordered composite media: II. Evaluation of bounds on the conductivity and bulk modulus of dispersions of impenetrable spheres," *Phys. Rev. B* **33**, 6428-6435 (1986).

- [16] D.A.G. Bruggeman, "Berechnung verschiedener physikalische Konstanten von heterogenen Substanzen, I. Dielektrizitäts-konstanten und Leitfähigkeiten der Mischkörper aus isotropen Substanzen," *Ann. Phys. (Leipzig)* **[5]**, 24, 636-679 (1935).
- [17] W.T. Doyle, "The Clausius-Mossotti Problem for Cubic Arrays of Spheres," *J. Appl. Phys.* **49**, 795-797 (1978).
- [18] R.C. McPhedran, personal communication (1986).
- [19] D.R. McKenzie, R.C. McPhedran and G.H. Derrick, "The Conductivity of Lattices of Spheres II. The Body Centred and Face Centred Cubic Lattices," *Proc. Roy. Soc. London A* **362**, 211-232 (1978).
- [20] R.C. McPhedran and D.R. McKenzie, "The Conductivity of Lattices of Spheres I. The Simple Cubic Lattice," *Proc. Roy. Soc. London, A* **359**, 45-63 (1978).
- [21] H.B. Levine and D.A. McQuarrie, "Dielectric Constant of Simple Gases," *J. Chem. Phys.* **49**, 4181-4187 (1968).
- [22] R. Guillian, "Variation de la Polarisation Diélectrique avec la Densité," *Ann. Physique (Paris)*, Ser. 11, **16**, 205-252 (1941).
- [23] J.C.R. Turner, "Two Phase Conductivity: The Electrical Conductance of Liquid-Fluidized Beds of Spheres," *Chem. Engineering Science*, **31**, 487-492, (1976); "Electrical Conductivity of Liquid-Fluidized Beds," *AIChE Symposium Series*, **69**, No. 128, pp. 115-122 (1973).
- [24] W.T. Doyle and I.S. Jacobs, "Pair Interactions in Artificial Dielectric Media," Abstract in *Bull. Am. Phys. Soc.* **32**, 830 (1987).